Measurement of Fast Electron Spin Relaxation Times with Atomic Resolution

Sebastian Loth,[1*] Markus Etzkorn,[2] Christopher P. Lutz,[1] D. M. Eigler,[1] Andreas J. Heinrich[1*]

Single spins in solid-state systems are often considered prime candidates for the storage of quantum information, and their interaction with the environment the main limiting factor for the realization of such schemes. The lifetime of an excited spin state is a sensitive measure of this interaction, but extending the spatial resolution of spin relaxation measurements to the atomic scale has been a challenge. We show how a scanning tunneling microscope can measure electron spin relaxation times of individual atoms adsorbed on a surface using an all-electronic pump-probe measurement scheme. The spin relaxation times of individual Fe-Cu dimers were found to vary between 50 and 250 nanoseconds. Our method can in principle be generalized to monitor the temporal evolution of other dynamical systems.

When a magnetic atom is placed in a solid or onto a surface, it can exchange energy and angular momentum with the local environment, giving a finite lifetime to its excited spin states. For non-itinerant (localized) electron systems, these interactions occur on the atomic length scale and on a time scale generally in the pico- to microsecond range. Magnetic resonance techniques are widely used to measure spin relaxation times (*1*), but achieving high spatial resolution of individual spins rather than ensembles has remained a challenge (*2*–*4*). Spin-polarized scanning tunneling microscopy (STM), by contrast, can probe static magnetic properties on the atomic scale, such as complex magnetic order (*5*), *g*-values (*6*), anisotropy (*7*, *8*) and exchange energies (*9*, *10*). However, the bandwidth of conventional STM current amplifiers (*11*) is insufficient to directly access typical spin relaxation times. Efforts to enhance the STM's temporal resolution through faster current amplifiers (*12*) or pulsed laser techniques (*13*, *14*) have so far lacked atomic spatial resolution.

Here we show that the combination of an all-electronic pump-probe scheme with a spin-sensitive contrast mechanism (*15*, *16*) allows the STM to measure electron spin relaxation times of individual atoms with nanosecond time resolution. In this pump-probe scheme (Fig. 1), we apply a strong voltage pulse (the pump pulse) across the tunnel junction to create spin excitations of the surface atom and a weaker voltage pulse (the probe pulse) to interrogate the state of the atom's spin at a time Δt after the pump pulse (*17*). Integrating the probe-pulse current over many pump-probe cycles and slowly varying Δt allows us to map out the average dynamical evolution of the atom's spin.

[1]IBM Research Division, Almaden Research Center, 650 Harry Road, San Jose, CA 95120, USA. [2]Institut de Physique de la Matière Condensée, Ecole Polytechnique Fédérale de Lausanne, CH-1015 Lausanne, Switzerland.

*To whom correspondence should be addressed. E-mail: lothseb@us.ibm.com (S.L.); heinrich@almaden.ibm.com (A.J.H.)

Atomic-scale structures having long spin relaxation times may have applications in information storage or quantum information processing (*18*). It was shown that large easy-axis magnetic anisotropy can lead to long spin relaxation times (*19*) that are sufficient for coherent spin manipulation (*20*). Fe atoms placed on a Cu_2N overlayer on a Cu(100) surface have shown considerable magneto-crystalline anisotropy (*8*). Cu_2N binds the Fe atoms in a polar-covalent network that enables large anisotropy and decouples the adatoms from the Cu conduction electrons (*10*, *21*, *22*), allowing Fe to retain its free atom spin of $S = 2$ (*8*). Here we increased the easy-axis anisotropy of an Fe atom by placing it adjacent to a Cu adatom (Fig. 2A). We probed the dimer using spin-excitation spectroscopy (Fig. 2B) and found the first excitation at a threshold voltage of $V_{thr} = 16.7$ mV, a factor of 4 higher than for the individual Fe atom. This indicates an unusually large easy-axis anisotropy, and indeed we find spin relaxation times that exceed 200 ns.

Spin excitations of the surface atom are driven by inelastic scattering of the tunneling electrons (*6*). In this process, the pump voltage must exceed the threshold voltage, V_{thr}, required to drive the atom's spin from the ground state to an excited state. In general, the magnetic orientation of an excited spin state will be different from that of the ground state. We can sense the orientation of the surface atom's spin by magneto-resistive tunneling with a spin-polarized tip (Fig. 1) (*17*). The tunnel current that flows during the probe pulse then depends on the projection of the surface atom's spin along the spin-polarization axis of the tip.

A pump-probe measurement of an Fe-Cu dimer at 0.6 K temperature and 7 T magnetic field is shown in Fig. 2C. In our experiments, we record the probe-pulse current, which can be expressed as the number of electrons per probe pulse, N. We plot $\Delta N = N(\Delta t) - N(-600\ \text{ns})$, the change in N with respect to its value when the probe pulse precedes the pump pulse, a condition in which the spin is in its ground state during the probe pulse. The behavior of ΔN for positive delay times reveals the dynamical evolution of the Fe-Cu dimer after the end of the pump pulse. Between pump and probe pulse, no voltage was applied that could disturb the free evolution of the surface atom's spin. We observe ΔN to be negative and to exponentially decay to zero as Δt is increased. ΔN is expected to be negative: In the ground state, the surface spin is aligned nearly parallel to the spin-polarization axis of the tip. Any spin excitation reduces the projection of the surface spin along the polarization axis of the tip and hence reduces the conductance of the tunnel junction. The exponential decay of ΔN is characteristic for a system with a single rate-limiting relaxation mechanism. Fitting an exponential to the time dependence of ΔN yields a relaxation time of $T_1 = 87 \pm 1$ ns.

To demonstrate that the observed exponential decay is indeed due to spin relaxation, we performed two control experiments. First, we repeated the measurement on the same Fe-Cu dimer but with a non–spin-polarized tip (Fig. 2C). We switched between spin-polarized and non–spin-polarized STM tips by means of the reversible transfer of a Mn atom from the surface to the apex of the tip (*15*). Without spin polarization of the tip, the conductance of the tunnel junction is insensitive to the orientation of the dimer spin, and we correspondingly observe ΔN to be zero. Second, we repeated the measurement with a spin-polarized tip but on a Cu adatom, which has no features in its spin excitation spectrum (Fig. 2B), consistent with having no net spin. As expected, we observe ΔN to be zero in this case (Fig. 2C).

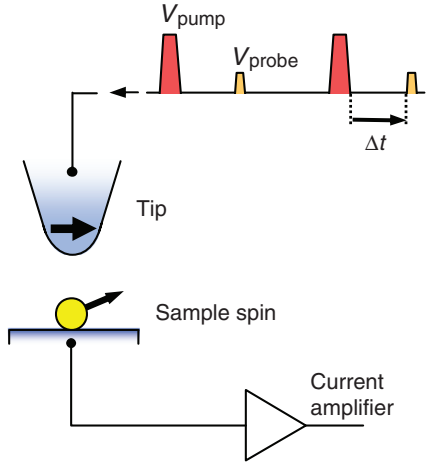

Fig. 1. Spin-sensitive pump-probe measurement scheme. The conductance of the STM tunnel junction varies according to the alignment of the sample spin with the tip spin. A series of fast voltage pulses with voltage V_{pump} for the pump pulse and V_{probe} for the probe pulse is sent to the tip. Measurement of the time-averaged probe-pulse current as a function of the delay time between the pulses, Δt, reveals the dynamical evolution of the sample spin.

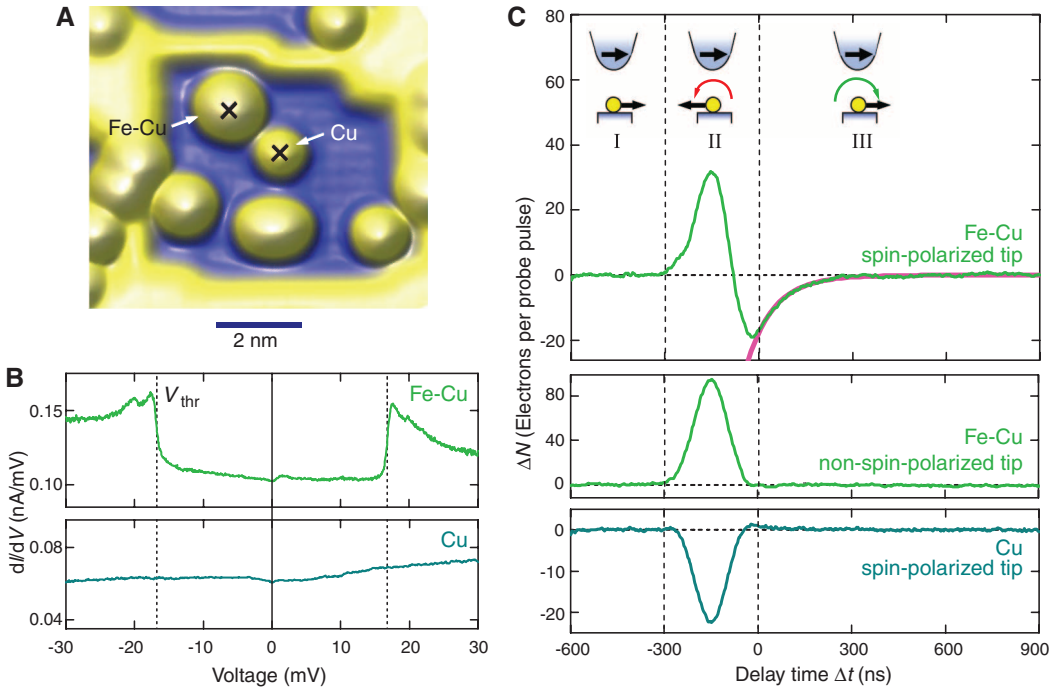

Fig. 2. Measurement of spin relaxation time. (**A**) STM topograph of an Fe-Cu dimer and a Cu adatom (yellow: high; blue: low). (**B**) Spin excitation spectra d*I*/d*V* versus voltage, of an Fe-Cu dimer and a Cu adatom measured with a non–spin-polarized tip at magnetic field $B = 7$ T. Steps in d*I*/d*V* indicate spin excitation energies. (**C**) Pump-probe measurements, ΔN versus Δt, at $B = 7$ T. Region I: probe pulse precedes the pump pulse; region II: pump and probe pulses overlap (fig. S1) (*17*); region III: probe pulse follows the pump pulse and senses the postexcitation dynamics of the system. Insets depict the relative orientation of tip and sample spins. For the Fe-Cu dimer (top panel) ΔN decays exponentially in region III, with a spin relaxation time of $T_1 = 87 \pm 1$ ns obtained from an exponential fit (magenta). Control experiments on the same Fe-Cu dimer but without spin sensitivity in the tip (middle panel) and on a Cu atom with spin-sensitivity in the tip (bottom panel).

We tested whether the pump-probe measurement was itself affecting the spin relaxation time and found that T_1 does not change under variation of the amplitude and widths of the pump and probe pulses and the tip-sample separation (Fig. 3B and fig. S2). However, the magnitude of the pump-probe signal, ΔN, depends strongly on the pump voltage, with a distinct onset at V_{thr}, below which the pump pulse does not lead to a detectable spin relaxation signal (Fig. 3A). This observation agrees with the spin excitation spectrum, where the first spin excitation is observed at the same threshold voltage (Fig. 2B). The polarity of the pump pulse is not crucial, but negative voltages help in exciting the Fe-Cu dimer's spin by spin-momentum transfer from the spin-polarized tip (*15*).

The pump-probe measurements corroborate the finding of large easy-axis magnetic anisotropy for the Fe-Cu dimers. Such anisotropy gives rise to a spin state distribution with two low-lying states, $|+2\rangle$ and $|-2\rangle$, that are separated by an energy barrier (Fig. 3C). In a magnetic field along the easy axis, $|+2\rangle$ is the ground state and $|-2\rangle$ a long-lived excited state. Excitation of the Fe-Cu dimer over the barrier starts with a transition from $|+2\rangle$ to $|+1\rangle$ and requires at least eV_{thr} energy (Fig. 3C, red arrow), which results in the threshold behavior found in the pump-probe measurement (Fig. 3A). Once excited to the $|+1\rangle$ state, successive excitations and de-excitations (Fig. 3C, light red arrows) are immediately possible as none require energy exceeding eV_{thr}. Upon termination of the pump pulse, the spin can be in any of the states but relaxes to either $|+2\rangle$ or $|-2\rangle$ on a time scale that is as yet too rapid for us to observe (*15*). The time-dependent signal recorded in the pump-probe measurement for $t > 0$ (Fig. 2C, region III) then corresponds to the relaxation from the long-lived $|-2\rangle$ state (Fig. 3C, green arrow). At 0.6 K the thermal energy is insufficient to relax over the energy barrier, and indeed no thermally activated relaxation is observed for temperatures between 0.6 and 10 K (fig. S3). Hence, the relaxation out of $|-2\rangle$ is likely due to magnetic tunneling (*23*, *24*), as we discuss next.

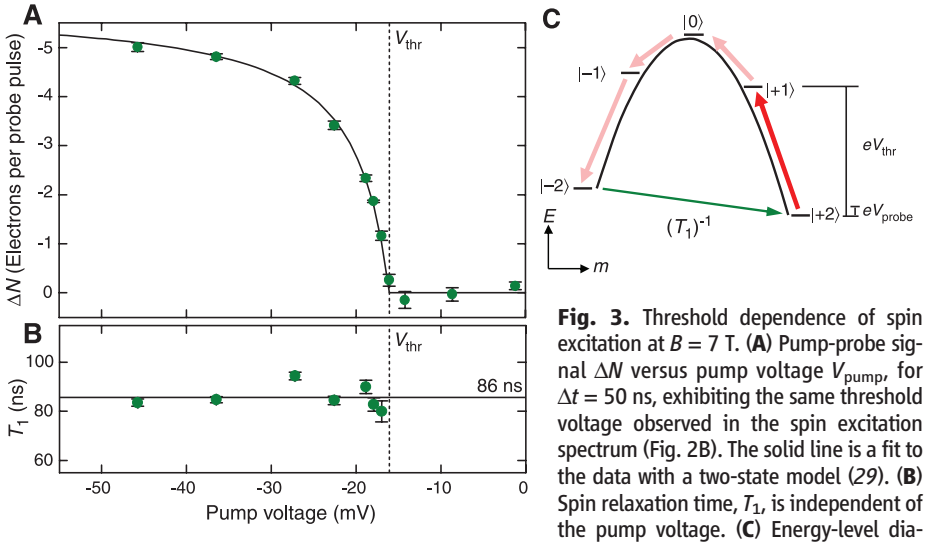

Fig. 3. Threshold dependence of spin excitation at $B = 7$ T. (**A**) Pump-probe signal ΔN versus pump voltage V_{pump}, for $\Delta t = 50$ ns, exhibiting the same threshold voltage observed in the spin excitation spectrum (Fig. 2B). The solid line is a fit to the data with a two-state model (*29*). (**B**) Spin relaxation time, T_1, is independent of the pump voltage. (**C**) Energy-level diagram of the spin states of the Fe-Cu dimer as a function of the magnetic quantum number, m. The measured relaxation time, T_1, corresponds to the $|m = -2\rangle \rightarrow |+2\rangle$ transition.

Figure 4A shows that ΔN decays as a single exponential for all values of magnetic field, but the relaxation time varies strongly with magnetic field. T_1 first grows with magnetic field, but declines rapidly above ~6 T (Fig. 4B). A similar non-monotonous field dependence of T_1 was recently observed for quantum tunneling of magnetization in molecular magnets (*19*). Finite transverse anisotropy makes magnetic tunneling possible for Fe-Cu dimers by mixing the $|-2\rangle$ and $|+2\rangle$ states. As the magnetic field is increased from zero, the Zeeman energy increasingly splits these states, which reduces the tunneling matrix element between them and thereby increases T_1 (*23*). The reduction in T_1 above 6 T indicates a nonzero angle between the magnetic field and the easy magnetic axis of the Fe-Cu dimer. A transverse component of the magnetic field increases mixing of the spin states and shortens T_1 (*25*).

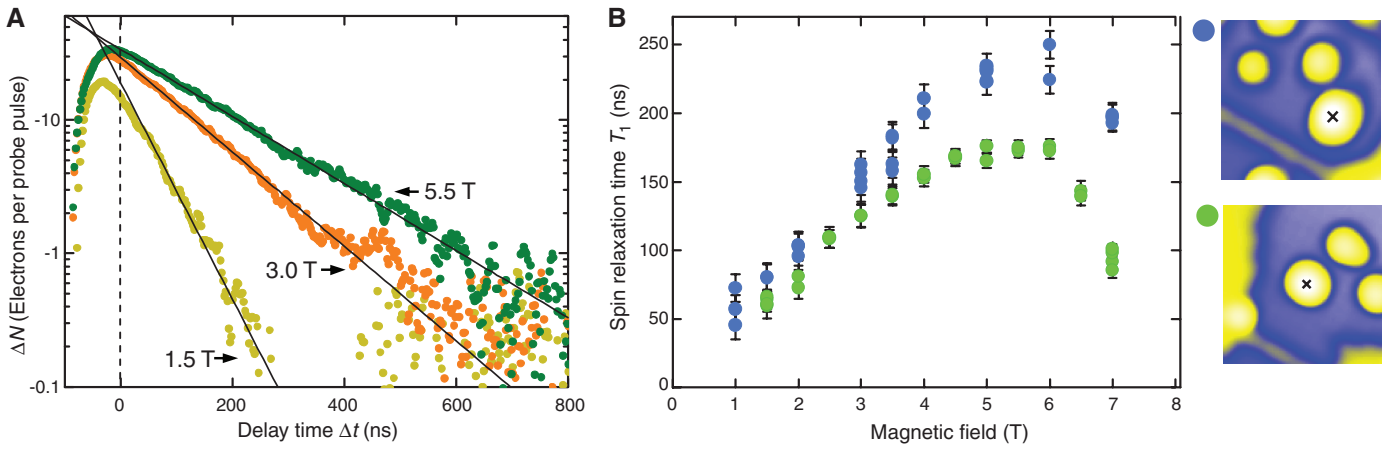

Fig. 4. Field and site dependence of the spin relaxation time. (**A**) Pump-probe measurements for different magnetic fields on an Fe-Cu dimer; solid lines are exponential fits. (**B**) T_1 as a function of magnetic field for the two Fe-Cu dimers shown in the accompanying 5-nm by 5-nm STM topographs.

One of the Fe-Cu dimers in Fig. 4B always exhibits a larger T_1 than the other. We speculate that this variation is due to differences in the nearby surface features as seen in the accompanying topographs. This observation emphasizes the capability of the all-electronic pump-probe technique presented here to resolve local variations in the spin relaxation time with atomic precision.

The pump-probe scheme we have described can be used to monitor the temporal evolution of any excitation provided (i) the excitation can be driven by tunneling electrons; (ii) the conductance of the tunnel junction exhibits a postexcitation time dependence; and (iii) the system evolves on an accessible time scale. Excitations fulfilling these requirements include long-lived vibrational excitations, conformational changes of molecules (*26*) such as in molecular motors (*27*), or fast localized heating (*28*). We emphasize that this pump-probe scheme can in principle be used to monitor the dynamical evolution of the excited state, not just its relaxation; with sufficient temporal resolution it should be possible to monitor the vibration of an atom or molecule and even the precession of a spin.

References and Notes

1. C. P. Slichter, *Principles of Magnetic Resonance* (Springer, Berlin and New York, 1996).
2. D. Rugar, R. Budakian, H. J. Mamin, B. W. Chui, *Nature* **430**, 329 (2004).
3. J. R. Maze *et al.*, *Nature* **455**, 644 (2008).
4. G. Balasubramanian *et al.*, *Nature* **455**, 648 (2008).
5. M. Bode *et al.*, *Nature* **447**, 190 (2007).
6. A. J. Heinrich, J. A. Gupta, C. P. Lutz, D. M. Eigler, *Science* **306**, 466 (2004).
7. N. Tsukahara *et al.*, *Phys. Rev. Lett.* **102**, 167203 (2009).
8. C. F. Hirjibehedin *et al.*, *Science* **317**, 1199 (2007).
9. X. Chen *et al.*, *Phys. Rev. Lett.* **101**, 197208 (2008).
10. C. F. Hirjibehedin, C. P. Lutz, A. J. Heinrich, *Science* **312**, 1021 (2006).
11. M. J. Rost *et al.*, *Rev. Sci. Instrum.* **76**, 053710 (2005).
12. C. Durkan, M. E. Welland, *Appl. Phys. Lett.* **80**, 458 (2002).
13. G. Nunes Jr., M. R. Freeman, *Science* **262**, 1029 (1993).
14. O. Takeuchi *et al.*, *Appl. Phys. Lett.* **85**, 3268 (2004).
15. S. Loth *et al.*, *Nat. Phys.* **6**, 340 (2010).
16. R. Wiesendanger, *Rev. Mod. Phys.* **81**, 1495 (2009).
17. Materials and methods are available as supporting material on *Science* Online.
18. M. N. Leuenberger, D. Loss, *Nature* **410**, 789 (2001).
19. D. E. Freedman *et al.*, *J. Am. Chem. Soc.* **132**, 1224 (2010).
20. A. Ardavan *et al.*, *Phys. Rev. Lett.* **98**, 057201 (2007).
21. T. Choi, C. D. Ruggiero, J. A. Gupta, *Phys. Rev. B* **78**, 035430 (2008).
22. F. Komori, S.-Y. Ohno, K. Nakatsuji, *Prog. Surf. Sci.* **77**, 1 (2004).
23. D. Gatteschi, R. Sessoli, J. Villain, *Molecular Nanomagnets* (Oxford Univ. Press, New York, 2006).
24. C. Sangregorio, T. Ohm, C. Paulsen, R. Sessoli, D. Gatteschi, *Phys. Rev. Lett.* **78**, 4645 (1997).
25. W. Wernsdorfer, R. Sessoli, *Science* **284**, 133 (1999).
26. K. Henzler-Wildman, D. Kern, *Nature* **450**, 964 (2007).
27. W. R. Browne, B. L. Feringa, *Nat. Nanotechnol.* **1**, 25 (2006).
28. B. Barwick, H. S. Park, O.-H. Kwon, J. S. Baskin, A. H. Zewail, *Science* **322**, 1227 (2008).
29. J. A. Gupta, C. P. Lutz, A. J. Heinrich, D. M. Eigler, *Phys. Rev. B* **71**, 115416 (2005).

30. We thank B. Melior for technical assistance. S.L., C.P.L., and A.J.H. acknowledge financial support from the Office of Naval Research, S.L. from the Alexander von Humboldt Foundation, and M.E. from European Science Foundation project FunSMARTs II.

Supporting Online Material

www.sciencemag.org/cgi/content/full/329/5999/1628/DC1
Materials and Methods
Figs. S1 to S3
References
Movie S1

30 April 2010; accepted 4 August 2010
10.1126/science.1191688

Optical Clocks and Relativity

C. W. Chou,* D. B. Hume, T. Rosenband, D. J. Wineland

Observers in relative motion or at different gravitational potentials measure disparate clock rates. These predictions of relativity have previously been observed with atomic clocks at high velocities and with large changes in elevation. We observed time dilation from relative speeds of less than 10 meters per second by comparing two optical atomic clocks connected by a 75-meter length of optical fiber. We can now also detect time dilation due to a change in height near Earth's surface of less than 1 meter. This technique may be extended to the field of geodesy, with applications in geophysics and hydrology as well as in space-based tests of fundamental physics.

Albert Einstein's theory of relativity forced us to alter our concepts of reality. One of the more startling outcomes of the theory is that we have to give up our notions of simultaneity. This is manifest in the so-called twin paradox (*1*), in which a twin sibling who travels on a fast-moving rocket ship returns home younger than the other twin. This "time dilation" can be quantified by comparing the tick rates of identical clocks that accompany the traveler and the stationary observer. Another consequence of Einstein's theory is that clocks run more slowly near massive objects. In the range of speeds and length scales encountered in our daily life, relativistic effects are extremely small. For example, if two identical clocks are separated vertically by 1 km near the surface of Earth, the higher clock emits about three more second-ticks than the lower one in a million years. These effects of relativistic time dilation have been verified in several important experiments (*2*–*6*)

Time and Frequency Division, National Institute of Standards and Technology (NIST), Boulder, CO 80305, USA.

*To whom correspondence should be addressed. E-mail: chinwen@nist.gov

Supporting Online Material:
Measurement of fast electron spin relaxation times with atomic resolution

Sebastian Loth[1], Markus Etzkorn[2], Christopher P. Lutz[1], D. M. Eigler[1] & Andreas J. Heinrich[1]

1) *IBM Research Division, Almaden Research Center, 650 Harry Road, San Jose, California 95120, USA*
2) *Institute of the Physics of Nanostructures, Ecole Polytechnique Fédérale de Lausanne (EPFL), CH-1015 Lausanne, Switzerland*

Experimental Setup:

We use an ultra-high-vacuum scanning tunneling microscope (STM) operating at an adjustable temperature of 0.6 K to 10 K. Magnetic fields up to 7 T were applied perpendicular to the sample surface. The fast voltage pulses are applied to the STM tip, but throughout this report we use the commonly employed convention of specifying the voltage of the sample with respect to the tip. For pump-probe measurements the tip-sample distance was fixed by setting the tunnel current to 1 nA at +10.0 mV sample voltage prior to opening the feedback loop.

The pump and probe voltage pulses were generated as continous pulse trains by a pulse pattern generator (Agilent 81110A). The pump-probe cycle was repeated every 2 μs and the probe pulse was chopped at 810 Hz. The pump and probe pulses were summed, attenuated by 20 dB and applied to the tip of the STM. The tunnel current is detected at the sample and fed to a current preamplifier (Femto DLPCA-200) with ~1 kHz bandwidth and from there to a lockin amplifier to selectively detect the 810 Hz component of the current corresponding to the tunnel current of the probe pulse. For the measurements shown in Fig. 2C, Fig. 4 and Fig. S2 the pump and probe pulses were 100 ns FWHM long with 50 ns linear-ramp rise and fall times. The amplitude of the pump pulse was −36.5 mV and thereby well above the −16.7 mV threshold for spin excitation. The probe pulse voltage was −4.0 mV leading to a baseline of N = 341 electrons per probe pulse as measured when the probe precedes the pump. The pulse parameters used in Fig. 3A are the same except for a lowered probe-pulse voltage of −1.2 mV and the variable pump-pulse voltage.

Spin-polarized STM measurements on Fe-Cu dimers:

The spin-polarized tip used in this work has one magnetic atom, Mn, attached to the otherwise non-magnetic Cu-coated apex. The magnetic atom that was used to create spin-polarization in the tip was picked up after the Fe-Cu dimers were assembled by vertical atom manipulation *(S1, S2)*. The magnetic moment of the attached atom is aligned parallel to the external magnetic field. This also determines the direction of the tip's spin-polarization *(S3)*. Since the magnetic atom at the tip apex is adsorbed directly on the metal surface of the tip (without a decoupling layer such as Cu_2N) much shorter spin lifetimes can be expected. Indeed we did not observe spin excitations for the tip atom and detect no dynamical change in the tip's spin polarization for all timescales that we can access experimentally.

In the present experiments, the magnetic field was applied perpendicular to the sample surface. Hence the tip's direction of spin polarization is also perpendicular to the sample surface. Since we see a strong signal in the spin sensitive pump-probe measurements of the Fe-Cu dimer (Fig. 2C) we conclude that the direction of its easy axis has a significant component parallel to the tip's spin polarization and therefore perpendicular to the sample surface. On the other hand the magnetic field dependence of the spin relaxation time (Fig. 4) indicates that magnetic field and easy-axis anisotropy are not completely parallel.
We note that a single Fe atom on the Cu binding site on Cu_2N has an easy axis that lies in the plane of the sample *(S4)*. In contrast to the single Fe atom, the anisotropy axis of the Fe-Cu dimer is rotated largely out of the sample plane. However, within the present data set we can not quantitatively determine the direction of the easy-axis of the Fe-Cu dimer.

Cross correlation of Pump and Probe pulse:

The linear slope in the differential conductance of the Fe-Cu dimer (see Fig. 2B) gives a quadratic (non-linear) shape to the $I(V)$-curve of the tunnel junction *(S5)*. Since the voltages for pump and probe pulse are summed, the voltage across the tunnel junction increases beyond V_{pump} or V_{probe} when pump and probe overlap. Hence the non-linearity of the tunnel junction creates a component of the current which is proportional to the cross correlation of the pump and probe voltages when the pulses overlap in time . This signal can be used to monitor the quality of the pulses directly at the tunnel junction (Fig. S1). Note that this cross correlation signal is present in all three panels of Fig. 2C which confirms that it is not of magnetic origin.

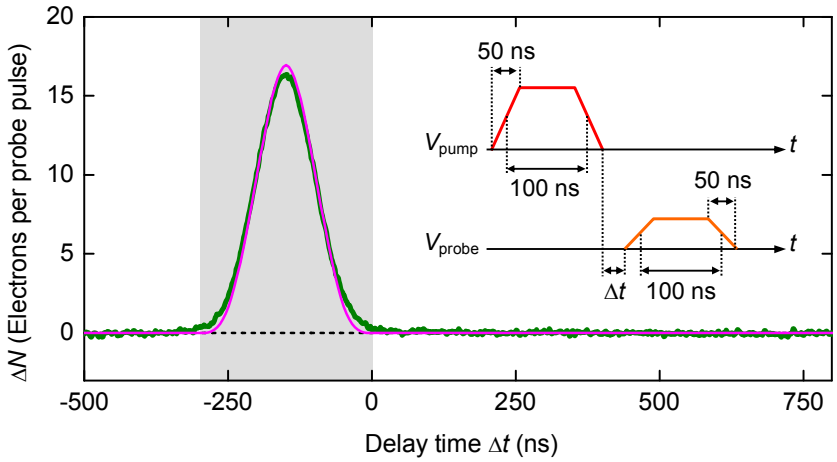

Figure S1. Pump-probe cross correlation. Green curve: ΔN vs. Δt of an Fe-Cu dimer, measured with the pump voltage well below the threshold for creating spin excitations. The gray region corresponds to the delay times in which overlap between the pump and probe pulses occurs assuming the ideal pulse shapes (see inset). A cross correlation term due to a non-linearity in the current vs. voltage characteristics of the tunnel junction (see Fig. 2B) gives rise to the peak seen in the gray region. Purple curve: Calculated ΔN vs. Δt for the experimentally derived values of pump amplitude $V_{\mathrm{pump}} = -8.7$ mV, probe amplitude $V_{\mathrm{probe}} = -1.2$ mV, average differential conductance of the tunnel junction $\mathrm{d}I/\mathrm{d}V(V = 0\ \mathrm{mV}) = 0.11$ nA/mV, average slope in the differential conductance $\mathrm{d}^2I/\mathrm{d}V^2 = -2.1$ pA/mV^2 and the pulse shapes shown in the inset. The baseline number of electrons per probe pulse is 218.

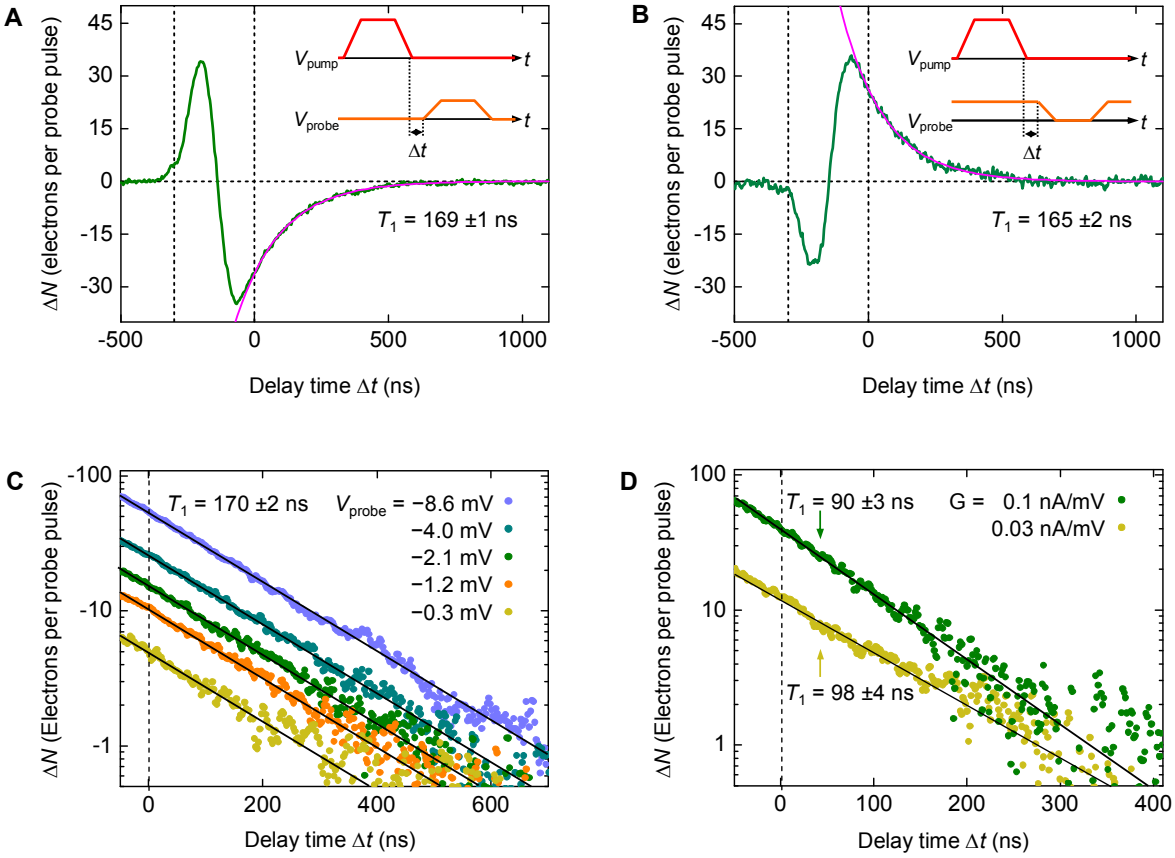

Figure S2. Additional control experiments demonstrating that the tunnel current during the probe pulse has no impact on the spin relaxation time. All measurements were performed on the Fe-Cu dimer represented with green dots in Fig. 4B. (**A**) Pump-probe measurement, ΔN vs. Δt, at $B = 5$ T with the pump and probe pulses having a width of 100 ns at FWHM and 50 ns linear-ramp rise and fall (see inset and above section *Experimental Setup*). The voltage of the probe pulse is $V_{probe} = -4$ mV. (**B**) Pump-probe measurement with the same conditions as in *(A)* but with an inverted probe pulse: A voltage of −4 mV was constantly applied except for a window of 100 ns at FWHM. As expected the measured signal is the inverse of that recorded in *(A)*. This scheme applies a probe pulse that is longer than 1 µs and demonstrates that the Fe-Cu dimer's spin relaxation is not affected by the duration of the probe pulse. (**C**) ΔN vs. Δt at $B = 5$ T with varying probe pulse voltage V_{probe}. The fitted spin relaxation time, T_1, is given by the slope of the black lines in the logarithmic plot. All curves are well fit by a single T_1, so the spin relaxation time is independent of V_{probe}. Together with the pump voltage dependence (Fig. 3B) this demonstrates that the electric field due to the voltage pulses (which is of the order of 10^6 V/cm for the largest voltages used here) does not affect T_1. (**D**) ΔN vs. Δt at $B = 7$ T with varying tip-sample separation identified by the tunnel junction impedance, G, at +10 mV. The exponential fit to the data shows only a slight variation in the measured lifetime that is within the uncertainty of the measurement. This indicates that the magnitude of tunnel current during the pump-probe measurement has no significant impact on the spin relaxation.

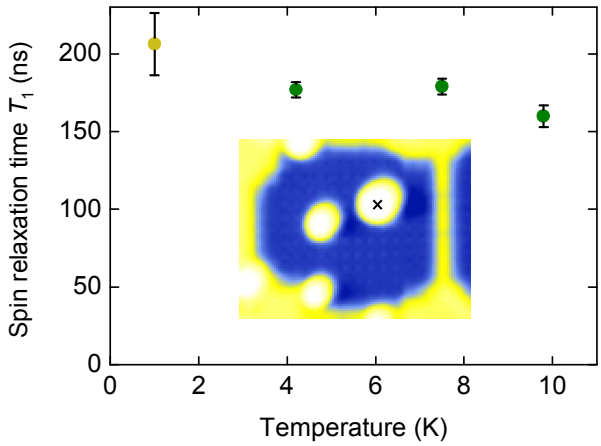

Figure S3. Temperature dependence of the spin relaxation time for an Fe-Cu dimer. For a thermally activated relaxation process a fast drop in T_1 at higher temperatures is expected. However, within the measurement accuracy, T_1 is essentially constant below 10 K. The drop at 10 K might indicate the beginning of a thermally-activated spin relaxation. In either case, at 0.6 K, where all measurements of the main text were recorded, spin relaxation can be attributed to a non-thermal process. The pump-probe measurements >1 K were recorded at 5.5 T magnetic field (green dots). The measurement at 1 K was at 4.0 T magnetic field and was extrapolated to 5.5 T using the measured magnetic field dependence of T_1 which resulted in a bigger uncertainty. Inset: 6.5 nm × 5.0 nm topograph of the Fe-Cu dimer.

References:

S1. C. F. Hirjibehedin, C. P. Lutz, A. J. Heinrich, Spin coupling in engineered atomic structures, *Science* **312**, 1021–1024 (2006).

S2. L. Bartels, G. Meyer, K.-H. Rieder, Controlled vertical manipulation of single CO molecules with the scanning tunneling microscope: A route to chemical contrast, *Appl. Phys. Lett.* **71**, 213–215 (1997).

S3. S. Loth *et al.*, Controlling the state of quantum spins with electric currents, *Nat. Phys.* **6**, 340 (2010).

S4. C. F. Hirjibehedin *et al.*, Large magnetic anisotropy of a single atomic spin embedded in a surface molecular network, *Science* **317**, 1199–1203 (2007).

S5. G. Nunes Jr., M. R. Freeman, Picosecond resolution in scanning tunneling microscopy, *Science* **262**, 1029–1032 (1993).

Caption for Supplemental Movie S1, manuscript No. 1191688:

Movie S1. Spatially resolved pump-probe measurement of four Fe-Cu dimers. **(Scene 1)** STM topograph of Fe-Cu dimers that were individually assembled on four Cu_2N patches (green: high; blue: low). Image size is 12 nm by 12 nm. **(Scene 2)** Sequence of pump-probe measurements plotting $\log(|\Delta N|)$ overlaid as color on the topograph for different delay times Δt (red: large signal; white: small signal). The time-dependent signal at $\Delta t > 0$ is localized at each Fe-Cu dimer and decays for increasing Δt. Schematic at left indicates the pulse sequence for each Δt. **(Scene 3)** Comparison of spatially resolved pump-probe measurements for the same Fe-Cu dimers at 4 T and 1 T magnetic field. **(Scene 4)** Spin relaxation times, T_1, for each Fe-Cu dimer as determined by exponential fit to the pump-probe data of (scene 2) and (scene 3). The variations in the T_1 times are likely due to variations in the nearby surface features.

Parameters of the pump-probe measurement: $V_{pump} = -35$ mV, $V_{probe} = -10$ mV, pulse duration 100 ns for the pump pulse and 60 ns for the probe pulse at FWHM with 10 ns linear rise and fall times, repetition of pump-probe cycle every 1.3μs.